# RIDGE BASED DECOMPOSITION OF COMPLEX BUILDINGS FOR 3D MODEL GENERATION FROM HIGH RESOLUTION DIGITAL SURFACE MODELS

H. Arefi [a], M. Hahn [b] and P. Reinartz [a]

[a] German Aerospace Center (DLR), Remote Sensing Technology Institute, D-82234 Wessling, Germany,
(hossein.arefi, peter.reinartz)@dlr.de
[b] Stuttgart University of Applied Sciences, D-70174 Stuttgart, Germany , michael.hahn@hft-stuttgart.de

## ABSTRACT

3D city models have a wide range of applications such as mobile navigation, urban planning, telecommunication, and tourism. The generation of high resolution Digital Surface Models (DSMs), in particular from airborne LIDAR data have found a major attraction of researchers in this field due to their high accuracy and high density of points. In this paper, a new approach is proposed for the generation of 3D models of buildings that are extracted from a high resolution DSM. Particularly the complex buildings containing several smaller building parts are discussed. The building parts are individually modeled by a projection-based method and merged to form the final 3D model. The following building parts are considered to be modeled in the proposed approach: (1) flat roof, (2) gable roof, (3) hipped roof, and (4) mansard-shaped roof buildings. The complex buildings are decomposed into several parts according to the number of existing ridge lines. The ridge line extraction begins with image reconstruction by geodesic morphology (Arefi and Hahn, 2005) extracting the pixels of the highest part of the building segment, i.e., local maxima. Next, a Random SAmple Consensus (RANSAC) (Hartley and Zisserman, 2004) based technique is used to fit straight lines to the ridge points. The pixels of the building part regarding to each ridge line are projected onto a plane which is defined based on ridge direction. According to the type of the roof, a 2D model is fitted to the projected points. The 2D model is converted back to 3D by extruding it orthogonally to the projection plane. After reconstructing 3D models for all building parts, they are merged to form the overall 3D model of the building.

## 1. INTRODUCTION

Generating automatic 3D models of buildings has become a more challenging problem particularly after appearance of high resolution Digital Surface Models (DSMs) provided by LIDAR sensor or from high resolution optical satellite images. In this context, providing a 3D CAD model which represents the overall shape of the building and containing the most significant parts has boosted many applications in the GIS area such as urban planning and mobile navigation systems. During the past few years, several algorithms have been proposed for 3D reconstruction of the buildings especially by employing high resolution DSMs. The approaches are mostly focusing on reconstructing the simple shaped buildings which contain a single gable roof (Weidner and Foerstner 1995, Maas 1999) or fitting prismatic models by flat roof buildings (Alharthy and Bethel, 2002). Segmentation based approaches are proposed by Geibel and Stilla (2000) and Rottensteiner and Jansa (2002) to find planar regions which determine a polyhedral model. Gorte (2002) employed another segmentation approach using TIN structure for the data. Segments are created by iterative merging triangles based on similarity measurements. Finally, the segmented TIN structure is transformed into a VRML model for visualization. Rottensteiner (2006) described a model for the consistent estimation of building parameters, which is part of 3D the building reconstruction. Geometric regularities were included as soft constraints in the adjustment of the model. Robust estimation can be then used to eliminate false hypotheses about geometric regularities. Tarsha Kurdi et al. (2007) have made a comparison between data- and model-driven approaches for building reconstruction. They state that the model-driven approach is faster and does not visually deform the building model. In contrast, the data-driven approach tends to model each building detail to obtain the nearest polyhedral model, but it usually visually deforms the real shape of the building. Since the modelling accuracy is strongly related to the technique used for building modelling, a meaningful comparison about the modelling precision of these two approaches is not possible.

In this paper, a new method is proposed which aims at simplifying the 3D reconstruction of the building blocks by dividing the model into several smaller ones corresponding to each building part. A CAD model containing four vertical walls plus the polygon faces on the roof regarding to the simple inclined or flat roof buildings defines a 3D model related to a building part. Next, a projection-based algorithm is employed to transfer the 3D points into the 2D space by projecting the corresponding pixels of each building part onto a 2D plane that is defined based on the orientation of the ridge line. According to the type of the roof, a predefined 2D model is fitted to the data and in the next step, the 2D model in extended to 3D by analyzing the third dimension of the points. A final model of the building block is defined by merging all the individual models and employing some post processing refinements regarding the coinciding nodes and corners to shape the appropriate model. The paper is organized as follows: In the second section, the proposed algorithm for the automatic generation of building models is explained in detail. Experimental investigation with testing the proposed algorithm on some high resolution DSMs is represented in the third section and finally, in the last section, the quality of the results is discussed.
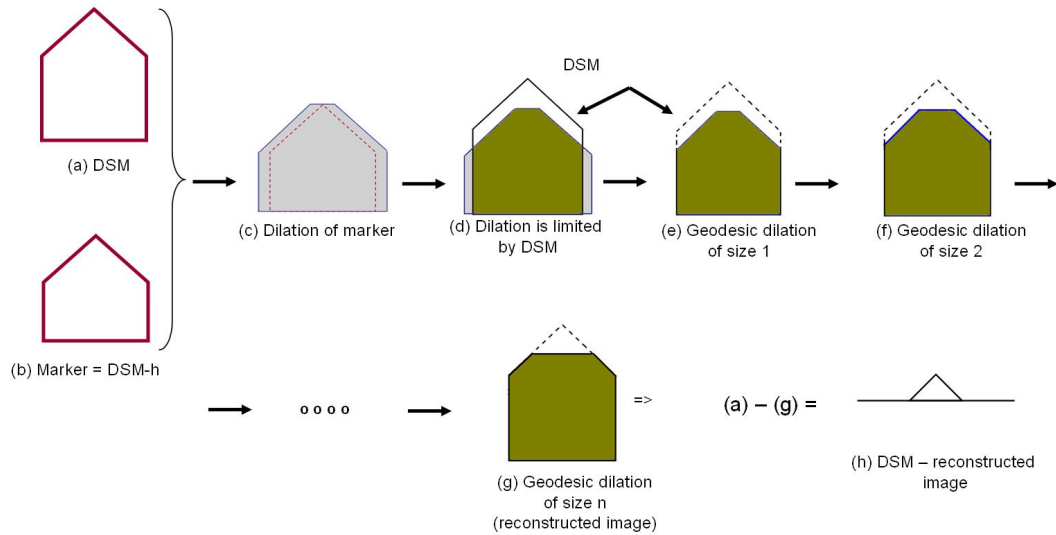
Figure 1. Geodesic morphological dilation for extracting local maxima of the building pixels

## 2. PROPOSED ALGORITHM

The proposed method for 3D modelling of the complex buildings is based on decomposition of the model into several simple shaped models. A building block as well as a complex one is decomposed by evaluating the roof top pixels or existing ridge lines into flat or gable shaped roofs. In order to simplify the 3D modelling of a building block, the ridge lines and their directions are used to extract individual building parts. A projection-based method is employed for simplification of the 3D modelling of the individual building parts. The proposed algorithm and the detailed processing steps are categorized in the following sections:

### 2.1 Extraction of local maxima

Extracting the ridge lines is the most effective part of the proposed reconstruction method in this paper. The quality of all the other steps is affected directly by the quality of the extracted ridge lines. In this paper, an algorithm based on Geodesic morphological dilation (Arefi, 2009) is employed to extract the local maxima pixels, which most probably belong to the roof top pixels or ridge lines. Figure 1 shows the principle of geodesic reconstruction by morphological dilation that is employed for extracting roof top pixels. Morphological operations based on geodesic distance employ two input images, namely mask and marker images. They allow the isolation of certain features within an image based on the manipulation of the mask and the marker image (Whelan and Molloy, 2001). Morphological reconstruction by dilation is based on the iterative application of dilations of the marker image until stability is reached, where the image

mask (here DSM) perpetually limits propagation or shrinking of the marker image.

We employ the geodesic reconstruction algorithm for potential ridge point extraction. For this purpose, the DSM image is chosen as mask image and accordingly a marker image generated by subtracting a small offset value from the DSM image. As shown in Figure 1, the marker image (cf. Figure 1b) is provided by subtracting an offset value h, e.g., 1m, from the DSM image (cf. Figure 1a). The following steps from (c) to (g) depict how the marker image (b) is reconstructed from the DSM (mask) based on geodesic dilation method. In order to build image reconstruction (cf. Figure 1g) the marker image is iteratively dilated (cf. Figure 1c) and then the result is masked by DSM. The product in this step called geodesic dilation of size 1 (cf. Figure 1e). The process continues until stability is reached (cf. Figure 1g) and image (marker) is reconstructed. The outcome in this step is geodesic dilation of size n or reconstructed image. In practice after each dilation, the point-wise minimum operation between DSM and dilated image provides geodesic dilation (cf. Figure 1d). The potential ridge points or roof top pixels are highlighted by subtracting the reconstructed image from the DSM (cf. Figure 1h).

### 2.2 Ridge line or flat roof segmentation

In this step the pixels which are extracted as local maxima in previous step are evaluated using Gaussian and mean curvature parameters (Besl, 1988). The roof top pixels are accordingly classified into the ridge and flat roof points. A further histogram-based classification process is implemented on ridge pixels before straight-line determination using
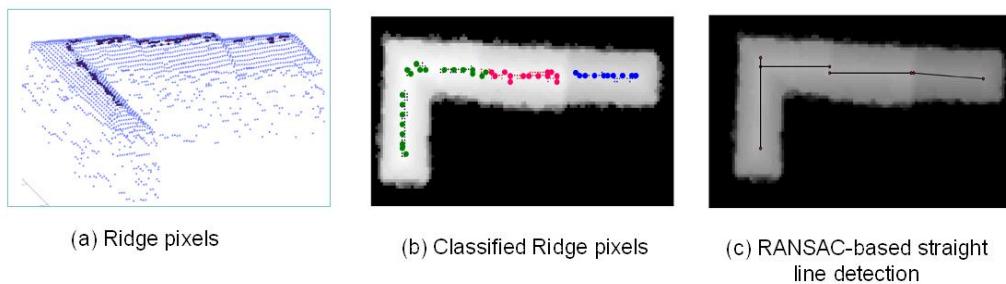


Figure 2. Fitting straight lines on classified ridge pixels using RANSAC algorithm

(a) Ridge points and lines

(b) Ridge points and lines; detail view

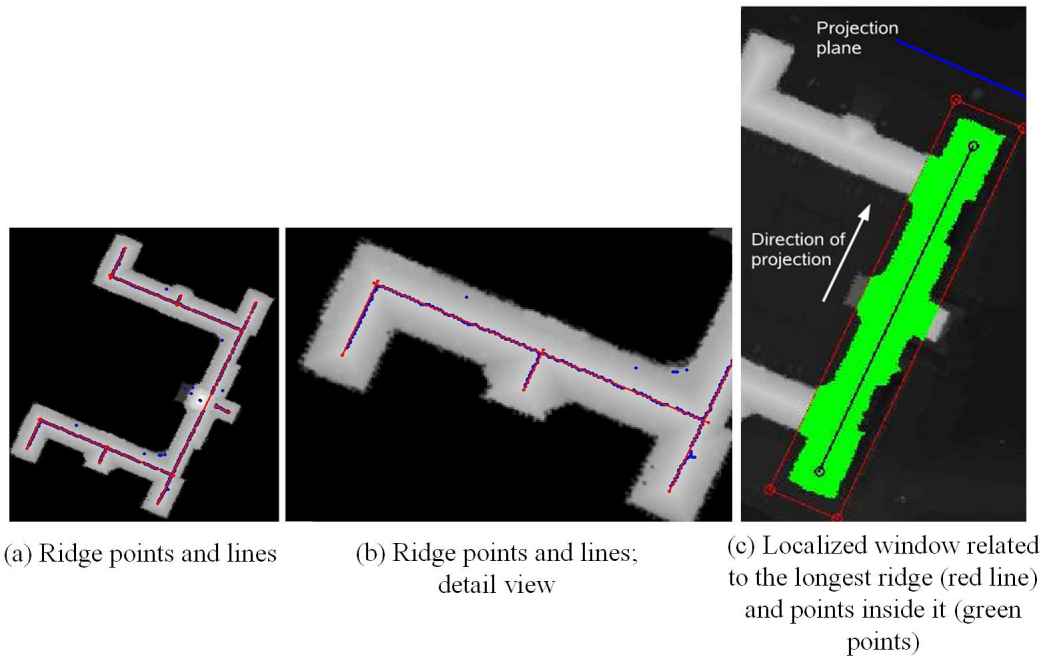(c) Localized window related to the longest ridge (red line) and points inside it (green points)

Figure 3. Detected ridge lines of Stuttgart Neuesschluss building and localized pixels belonging to the longest ridge line (green points)

RANSAC-based algorithm (Hartley and Zisserman, 2004). It is shown empirically that in some cases ridge lines are situated on very close height levels and RANSAC has difficulties to detect the individual lines correctly. Figure 2a illustrates the classified ridge pixels located on building roof as black dots. As shown in Figure 2b, the ridge pixels belong to the ridge lines in three different height levels which are classified as green, red, and blue points using histogram analysis of the points. RANSAC-based line fitting is employed afterward to iteratively extract corresponding ridge lines (cf. Figure 2c). The quality of RANSAC-based line fitting is directly related to the quality of the extracted points as ridge. Figure 2c shows that the extracted ridge lines are not exactly align to each other and this is due to quality of the extracted points as ridge. The location and direction of the ridge lines will be modified in the next steps while analyzing the points for 2D model fitting.

**2.3 Localization and extraction of building parts**

Proposed 3D reconstruction algorithm of the buildings from high resolution DSMs assumes that a building part exists according to each ridge line. Therefore, for each ridge line and the pixels locating in its buffer zone, a 3D model is fitted. In order to extract the corresponding pixels to each ridge line, a rectangle is defined parallel to the ridge line. In this localization step, the distance of the ridge line to the sides of the rectangle is defined based on the length of the ridge line (cf. red rectangle in Figure 3c). Next, the points located inside the rectangle are extracted by means of points-in-polygon method (cf. green dots in Figure 3c). Figure 3a and 3b visualize the potential ridge points (blue dots) remained after classification step using Gaussian and mean curvature parameters. Corresponding ridge lines detected by RANSAC are superimposed by red lines. Figure 3b shows the quality of extracted lines in zoomed view as well. As shown, few number of blue points that are wrongly classified as ridge points are remained unused. Those points are rejected during straight line detection due to sparseness and that the lines defined by them are not accepted because of

few number of obtained inliers in RANSAC processing (Hartley and Zisserman, 2004). A rectangle parallel to the longest ridge direction and around it is defined and corresponding building points inside it are extracted and highlighted as green points in Figure 3c.

**2.4 Projection of 3D points onto a plane and 2D model fitting of walls**

In this step, first a projection plane perpendicular to the ridge line direction is defined (cf. blue line if Figure 3c) and then all the localized points are projected onto this plane. The overall aim in this step is to look from the front view of the building part defined by the ridge direction and extract the 2D model related to the front- and back-side of the building part that take maximum support of the pixels.
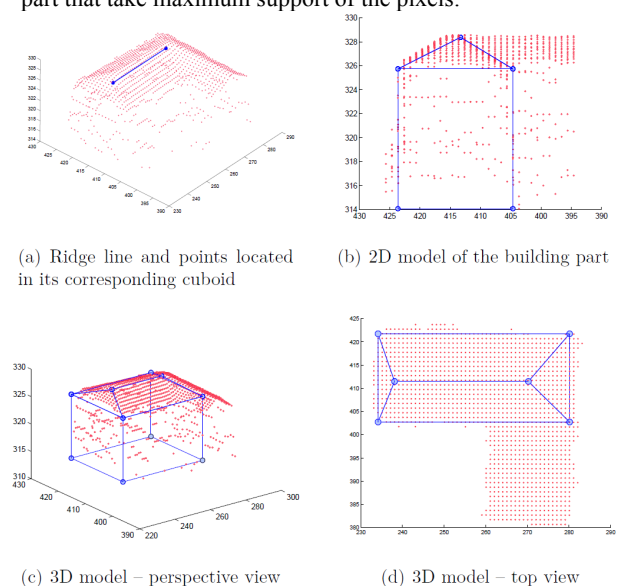


(a) Ridge line and points located in its corresponding cuboid

(b) 2D model of the building part

(c) 3D model – perspective view

(d) 3D model – top view

Figure 4. Modelling steps of building part in 2D and 3D spaces

(a) Ridge line computed by RANSAC – orientation correction = 0

(b) Orientation correction = $-0.095\ rad$

(c) Orientation correction = $0.1\ rad$

(d) Orientation correction = 0 $rad$ – cf. a

(e) Orientation correction = $-0.095\ rad$ – cf. b

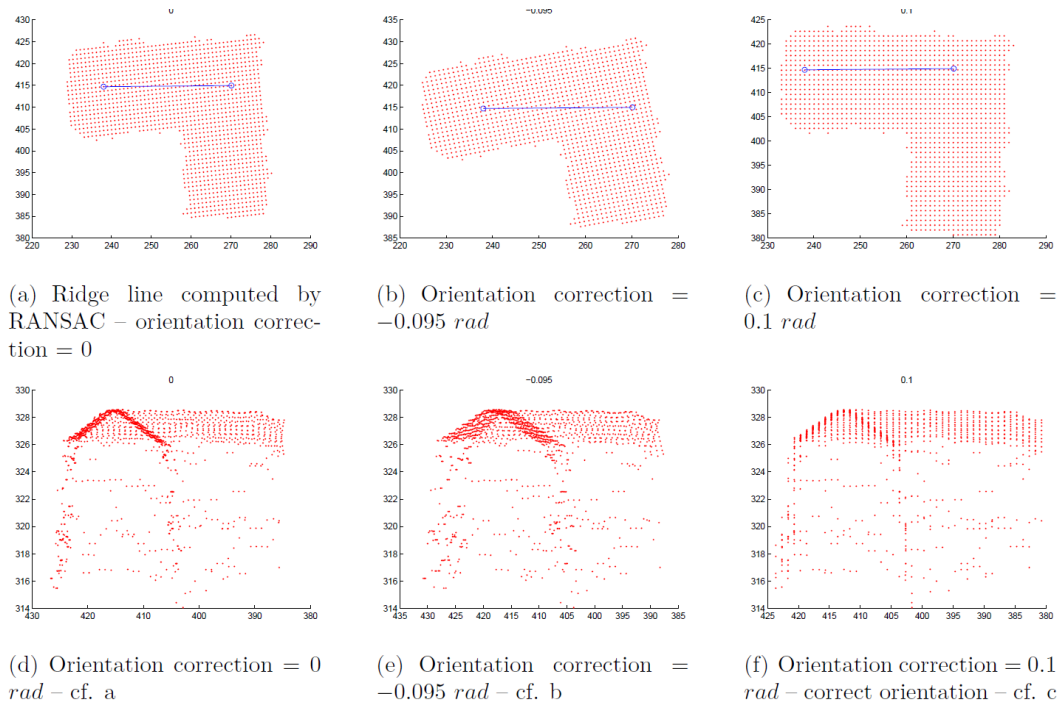(f) Orientation correction = 0.1 $rad$ – correct orientation – cf. c

Figure 5. Correction of the main orientation by iterative rotation of the localized points, computing the number of cells containing points in the 2D projection (bottom row)

For this intention, two vertical lines relating to the walls and two inclined lines relating to the roof faces are defined (cf. Figure 4b).The quality of the 2D model in this step depends on the existing a sufficient number of height points relating to each side of the wall. It is common in complex buildings that the number of supporting height points at least for one side of building part is not sufficient to be able to extract corresponding vertical line. To cope this problem a vertical line which is located symmetrically to the side with more supported points is defined. Hence, the algorithm in this step only extracts the side walls having equal distances to the ridge position.

As explained in Section 2.2, the extracted ridge lines using RANSAC algorithms related to the L-shaped building visualized in Figure 2c are not aligned to each other and should be corrected. In this step, an optimization procedure is performed on all extracted ridge lines. The optimization is based on the assumption that a correct ridge line produces the maximum density of the point distribution in the 2D view. I.e., the number of cells containing points in the 2D projection (cf. Figure 4b) is minimum if the direction of the ridge line is exactly parallel to the orientation of the building part. To obtain a high accuracy for the orientation, the localized points are rotated in small steps, e.g., 0.005 $rad$ (ca. 0.3°), and the number of cells, e.g., with 1m size, which contain points in the 2D view is counted. The local orientation with the minimum number of cells is added to the orientation of the ridge line, resulting into an accurate orientation of the building part. Figure 5 represents the correction procedure of a sample ridge line. It proves that a rotation of 0.1 $rad$ provides the minimum number of cells containing points in 2D projection.

Using the correct orientation, the location of the ridge line is refined by moving left and right locating the position with the maximum number of support points (cf. Figure 6).

## 2.5 Extension of 2D model in 3D space

In this Section the extension of the building part in the other direction, i.e., orthogonal to ridge orientation is defined. The 2D model is converted back to 3D by extruding it orthogonally to the projection plane. The 3D model consists of four walls plus one to four roof planes: two inclined planes in addition to two vertical triangular planes for a gable roof, and four inclined planes for a hipped roof (cf. Figure 4c).



(a) Points *(red)* corresponding to Figure 7.22(f) and position of ridge line *(blue circle)*

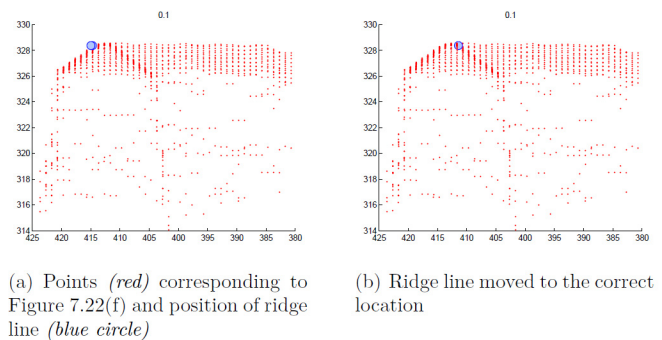(b) Ridge line moved to the correct location

Figure 6. Correction of the ridge line location by iteratively shifting the line left and right to find the position with the maximum number of support points

## 2.6 Modelling of flat or mansard shaped building parts

If a building part contains a flat or mansard shaped roof, automatically another technique for modelling is used: local maxima are classified into ridge points and flat roofs using a roundness criterion. The points at the boundary of the flat roof segment are analyzed if the building part has a flat or a mansard shaped roof. Minimum Bounding Rectangle (MBR) fitted to the building part defines the orientation of the building. If the building has a flat roof, the roof polygon is defined by MBR and accordingly a cuboid model is shaped. If the roof is mansard shaped, another rectangle inside and

parallel to the MBR is fitted to the flat part and the 3D model is formed.

### 2.7 Merging 3D models

After reconstructing 3D models for all building parts, they are merged to form the overall 3D model of the building. Figure 5 displays a building model produced by merging eight building parts. The eight ridge lines lead to eight parametric building models with hipped roofs. After combining the models, an overall 3D model is provided. For nodes of the building parts which have to be merged because they represent, e.g., the same corner of the building, the average value is determined. As shown in Figure 8, intersections might need to be refined for not rectangular building parts. To refine the two inconsistent nodes, the distances between the original LIDAR data points and each eave line are calculated. For each eave line, closest points, i.e., having a distance less than a certain threshold, are extracted. Using these supporting points, the eave lines are extended (or shortened) from both sides to the last point. For nodes generated from more than one vertex, the average is used.
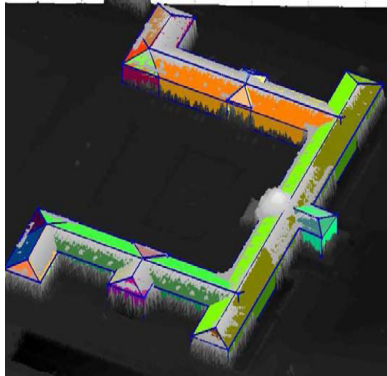


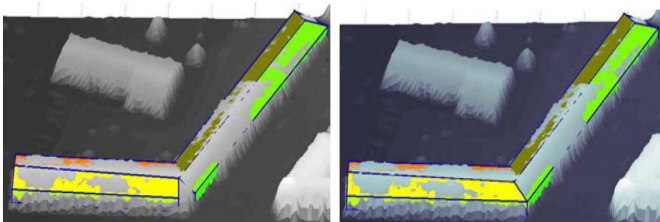Figure 7. 3D model after merging individual models



Figure 8. An example for projection-based building modelling with building parts intersecting at a non-orthogonal angle before (left), and after (right) adjusting the nodes

### 2.8 Comparison to the ground plan and adding flat roof building parts

By comparison between the overall boundaries of the 3D building models and the building ground plan, the corresponding indentation and protrusion regions can be detected. The overall area of the building block is subtracted from the corresponding area for the parametric models. This is done by subtraction a binary image that highlights the internal pixels of the building from the corresponding binary image of the parametric models. The positive pixels belong to protrusions and the negative pixels relate to indentations.

The regions provided by connected components labeling are analyzed and small regions are eliminated. An MBR is adapted to each remaining region after smoothing the regions using morphological closing. For protrusion, a cuboid-shaped 3D model is generated and the average of the heights of the internal points is used as building height. Although, this does not mean that the protrusion parts have always flat roof, but since their corresponding roof types cannot be distinguished by the proposed algorithm, a simple cuboid shaped model is fitted to the points. The corresponding MBR polygon nodes of indentation and protrusion regions are included in the overall 3D model. Finally, the inclinations of the building roofs are adapted after including the indentation nodes (cf. Figure 9).
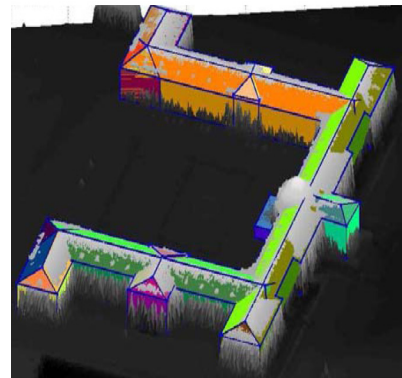


Figure 9. 3D model extended by a protrusion and two indentations

## 3. EXPERIMENTAL RESULTS

The algorithm proposed in this paper is tested and evaluated with high resolution DSM data. The DSM is generated from airborne LIDAR sensor. The data is captured by the TopScan company (TopScan, 2010), from the city of Stuttgart, Germany. A regularly spaced elevation grid is derived by means of spatial interpolation of the raw 3D points. A 0.5m point spacing is chosen for the elevation grid. The result and evaluation have been provided about the 3D building models possibly with tilted roofs. They are generated based on the analysis of the 3D point cloud in projection planes.

Figure 10 represents the processing results of 3D building reconstruction of two buildings that are contained several building parts. As discussed the algorithm is sensitive to the quality of the extracted ridge lines. In Figure 10a the location of several small ridge lines regarding the dormers above the roof are highlighted after local maxima extraction procedure. Since all these points are situated with small distances to a long ridge line, the RANSAC-based method could not generate any line relating to these points. On the other hand there exists another small ridge line but not located in the buffer zone of any longer ridge line which is correctly detected by RANSAC. Figures 10d to 10f correspond to a building comprising three ridge lines located in different height level. In all the 3D models illustrated in this paper, i.e., Figures 7, 8, 9, 10c, and 10f, the gray colour belongs to the original height data and representing this colour inside the model means that the generated 3D model in that point is below the original height point in DSM.
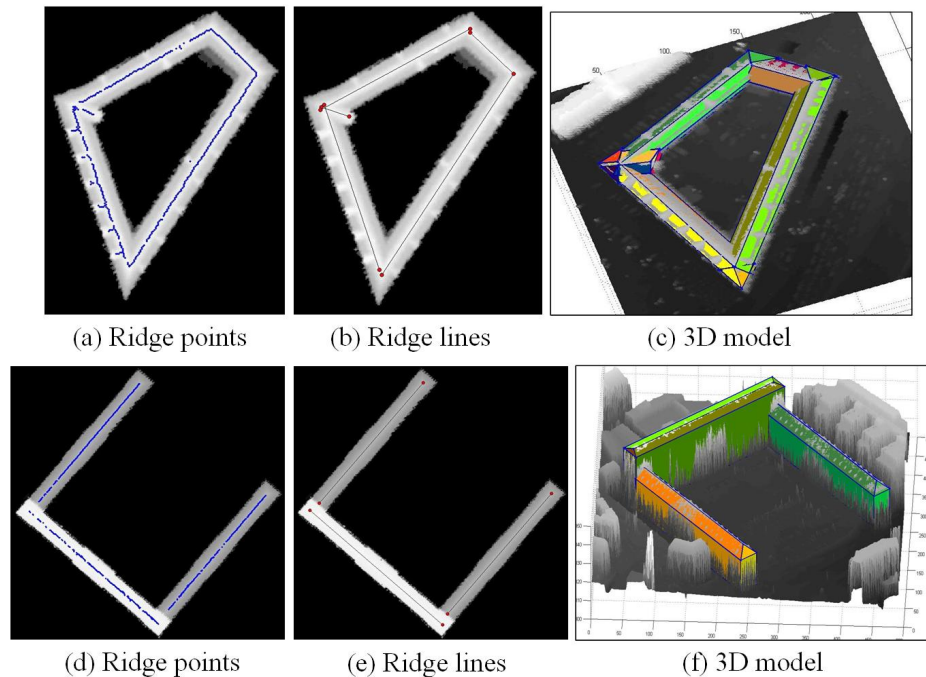
(a) Ridge points     (b) Ridge lines     (c) 3D model

(d) Ridge points     (e) Ridge lines     (f) 3D model

Figure 10. Proposed algorithm tested on two other buildings containing several building parts

## 4. DISCUSSION OF RESULTS

The quality of the 3D building models generated by means of the proposed algorithm is discussed as follows:
(1) The points are projected onto the 2D plane based on the direction of the ridge line. Therefore, the quality of the model is directly related to that of the detected ridge line. The initial ridge points are detected using geodesic dilation and are evaluated based on curvature values. (2) RANSAC-based ridge line detection is a sensitive process to extract the straight line representing the ridge line of the building in the correct orientation. The parameters of RANSAC, particularly the threshold for the distance to accept points as inliers, have to be carefully tuned. On one hand, it should be large enough to extract not too many straight lines, but on the other hand, it should be small enough to separate ridge lines situated at a small height difference, as can be seen in Figure 2. Thus, to avoid having to deal with ridge lines located very close to each other, they are classified in advance using histogram analysis (cf. Figure 2b). (3) The orientation of the building part could be optimized by iteratively rotating the points thought to belong to the building and counting the number of cells containing points in the 2D projection (cf. Figure 5). The locations of the ridge lines could also be optimized by moving them left and right and counting the number of supporting points (cf. Figure 6). (4) A mansard shaped building has been modeled after classifying the roof top pixels as partially flat and partially inclined. Two parallel MBR define the roof faces.

## REFERENCES

Alharthy, A. and Bethel, J., 2002. Heuristic filtering and 3D feature extraction from LIDAR data, International Archives of Photogrammetry, Remote Sensing and Spatial Information Sciences, Volume 34 (3A), 29 – 34.

Arefi, H. and Hahn, M., 2005. A morphological reconstruction algorithm for separating off-terrain points from terrain points in laser scanning data, International Archives of Photogrammetry, Remote Sensing and Spatial Information Sciences, Volume 36 (3/W19).

Arefi, H., 2009. From LIDAR Point Clouds to 3D Building Models, PhD thesis, University of Bundeswehr Munich, http://www.pf.bv.tum.de/pub/2009/arefi_phd09_the.pdf

Besl, P. J., 1988. Surfaces in Early Range Image Understanding, PhD thesis, University of Michigan.

Geibel, R. and Stilla, U., 2000.: Segmentation of laser-altimeter data for building reconstruction: Comparison of different procedures, International Archives of Photogrammetry and Remote Sensing and Spatial Information Sciences, Volume 33 (B3), 326 – 334.

Gorte, B., 2002. Segmentation of TIN-structured surface models, International Archives of Photogrammetry and Remote Sensing and Spatial Information Sciences, Volume 34 (4).

Hartley, R. and Zisserman, A., 2004. Multiple view geometry in computer vision, Cambridge University Press, Cambridge, UK.

Maas, H.-G., 1999. Fast determination of parametric house models from dense airborne laserscanner data, International Archives of Photogrammetry, Remote Sensing and Spatial Information Sciences, Volume 32 (2W1), 1 – 6.

Rottensteiner, F. and Jansa, J., 2002. Automatic extraction of buildings from LIDAR data and aerial images, International Archives of Photogrammetry, Remote Sensing and Spatial Information Sciences, Volume 34, 569–574.

Rottensteiner, F., 2003. Automatic Generation of High-quality Building Models from Lidar Data. IEEE Computer Graphics and Applications, 23(6):42–50, November/December 2003

Rottensteiner, F., 2006. Consistent estimation of building parameters considering geometric regularities by soft constraints, International Archives of Photogrammetry, Remote Sensing and Spatial Information Sciences, Volume 36 (3), 13 – 18.

Tarsha Kurdi, F., Landes, T., Grussenmeyer, P. and Koehl, M., 2007, Model-driven and data-driven approaches using LIDAR data: Analysis and comparison, International Archives of Photogrammetry, Remote Sensing and Spatial Information Sciences, Volume 36 (3-W49A), 87 – 92.

TopScan, 2010. TopScan GmbH, http://www.topscan.de/ : Last access February 2010

Weidner, U. and Förstner, W., 1995. Towards automatic building extraction from high resolution digital elevation models, ISPRS Journal of Photogrammetry and Remote Sensing, 50: 38 – 49.

Whelan, P. F. and Molloy, D. ,2001. Machine Vision Algorithms in Java: Techniques and Implementation, Springer Verlag New York, Inc., Secaucus, NJ, USA.